Patterned Differentiation of Individual Embryoid Bodies in Spatially Organized 3D Hybrid Microgels

By *Hao Qi, Yanan Du, Lianyong Wang, Hirokazu Kaji, Hojae Bae,* and *Ali Khademhosseini**

The capacity of embryonic stem cells (ESCs) to differentiate into virtually any cell type opens tremendous opportunities to generate renewable cell source for tissue engineering and regenerative medicine.[1,2] To implement ESCs as cell source for regenerative medicine, major challenge is to direct their differentiation to specific lineages with temporal and spatial control, mimicking the developmental processes *in vivo*.[3] Embryogenesis is a highly programmed process that results in polarized embryonic structures with proximal-distal and anterior-posterior axis.[4] The embryonic polarity is first established during gastrulation as patterned cellular differentiation occurs to yield spatially distinct cell types in embryo.[5] This patterning is governed by various intrinsic and extrinsic cues (such as soluble factors and extracellular matrix) presented in an asymmetrical manner. For example, during implantation, the embryo is partially embedded into endometrium in the uterus of mother. The contact between embryo and uterus induces the formation and development of polar trophectoderm complex in embryo with neo-vascularization for establishment and maintenance of connection with mother.[6]

One of the most widely-used approaches to promote differentiation of ESCs *in vitro* is by formation of three-dimensional (3D) aggregates, called embryoid bodies (EBs). EBs give rise to three primary germ layers: ectoderm, mesoderm, and endoderm which recapitulate the early embryonic development.[2] Despite the presence of cells from all three-germ layers in differentiated EBs, stochastic patterning and developmental noise are found during EB development resulting in uncontrolled spatial distribution of the differentiated cells.[7] Therefore, regulation of EB differentiation with defined polarities, which can imitate the patterned differentiation of primordial cells within an embryo, remains a challenge.

Microscale technologies enable unprecedented ability to control the cellular microenvironment, which can potentially provide solutions for addressing the challenges in recreating EB polarities.[1,8,9] In embryos, morphogens and extracellular matrices provide spatially oriented instructive cues for governing cellular differentiation.[3] The effects of soluble factors on recreating EB polarities *in vitro* have been demonstrated by using microfluidics.[10,11] For example, by taking advantage of the laminar flow in the microfluidic channel vascular endothelial cell growth factor (VEGF) was exposed to one side of an individual EB to result in patterned differentiation into endothelial lineage. One drawback of this approach was that the cells cultured on 2D substrates spread on the surface and lost their 3D geometry.

Despite advances in using materials for directing ESC differentiation,[9] the effectiveness of microengineered biological matrices on the formation of EB polarities has not been investigated. To address this issue we developed a novel microscale methodology to fabricate hybrid 3D microengineered hydrogels (microgels), containing two neighboring microscale hydrogels with disparate bioactivities. We hypothesized that the hybrid microgels can offer 3D asymmetrical microenvironments to direct the formation of EBs with engineered polarities. To test this hypothesis, we embedded individual EBs at the interface between the hybrid microgel with each half or quarter of each EBs exposed to different microenvironments. We used photocrosslinkable gelatin methacrylate (GelMA) and poly(ethylene glycol) diacrylate (PEG)[12] as example hydrogels to demonstrate the feasibility and effectiveness of spatially organized 3D matrices on the formation of EB polarities. We showed that EBs made from mouse ESCs exhibited developmental polarities with patterned vasculogenic differentiation induced by the GelMA/PEG hybrid microgels. More interestingly, the vasculogenic differentiation of individual EBs induced by the asymmetrical ECM was shown to be an orchestrated process with potential cross-talks between different portions of the EB exposed to different microenvironments.

Encapsulation of individual EBs into GelMA/PEG hybrid microgels was performed within a microwell array by using the combination of micromolding and photolithography techniques

[*] Dr. H. Qi, Dr. Y. Du, Dr. L. Wang, Dr. H. Kaji, Dr. H. Bae, Prof. A. Khademhosseini
Center for Biomedical Engineering
Department of Medicine
Brigham and Women's Hospital
Harvard Medical School, Boston, MA, 02115 (USA)
Telephone: 1 – 617-768 — 8395
Fax: 1 – 617-768 — 8477
E-mail: alik@rics.bwh.harvard.edu
Dr. H. Qi, Dr. Y. Du, Dr. L. Wang, Dr. H. Kaji, Dr. H. Bae, Prof. A. Khademhosseini
Harvard-MIT Division of Health Sciences and Technology
Massachusetts Institute of Technology
Cambridge, MA, 02139 (USA)
Dr. Y. Du
Biomedical Engineering
School of Medicine
Tsinghua University, Beijing (China)
Dr. L. Wang
Key Laboratory of Bioactive Materials
Ministry of Education
College of Life Science
Nankai University, Tianjin (China)
Dr. H. Kaji
Department of Bioengineering and Robotics
Graduate School of Engineering
Tohoku University, Sendai (Japan)

DOI: 10.1002/adma.201002873

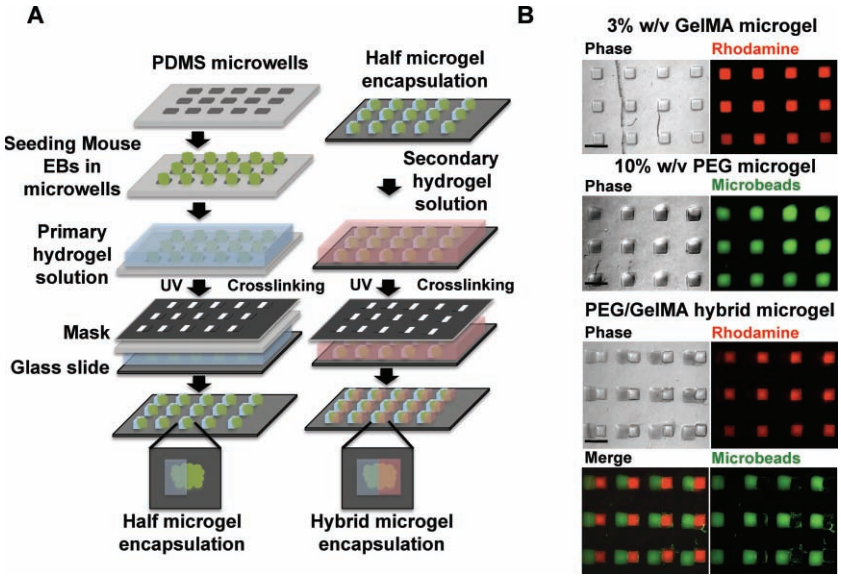

Figure 1. Fabrication of GelMA/PEG 3D hybrid microgels. (A) Schematic diagram of the process for fabricating GelMA/PEG hybrid microgels around individual EBs. Each half of individual EBs was successively encapsulated in PEG and GelMA microgel by photolithography. Photomasks were used to control the size of microgels. (B) Phase contrast and fluorescence images of a uniform array of GelMA microgels (top), PEG microgels (middle) and GelMA/PEG hybrid microgels (bottom). PEG and GelMA microgels were laden with green fluorescent microbeads and Rhodamine conjugated streptavidin, respectively. Scale bar: 1000 μm.

(**Figure 1A**). Individual EBs (~400 μm in diameter) were formed in hanging drops and seeded in PDMS microwell array with one EB per square microwell (500 μm(width) × 500 μm(length) × 450 μm(height)). Each half of the GelMA/PEG hybrid microgels was fabricated sequentially to encapsulate the EB within the microwell by controlled photocrosslinking through photomask with appropriate patterns (Figure 1A). The photomask was aligned with microwell array (covered by a glass slide) so that only half of a microwell containing the pre-polymer solution was exposed to the light. The GelMA half of the hybrid microgels was first formed on the glass slides followed by the formation of the second half made from PEG. The encapsulated EBs could be harvested by detaching the glass side from the microwell arrays. As shown by fluorescence staining in Figure 1B, homogeneous GelMA or PEG microgel arrays or hybrid GelMA/PEG microgel array were fabricated respectively. The hybrid microgel arrays contained 3D interconnected GelMA (red) and PEG (green) microgels without excessive overlapping with each other.

Upon the establishment of the microengineering approach for fabricating 3D hybrid microgel array, we investigated the effect of various properties of GelMA or PEG on EB differentiation. In particular we attempted to optimize the concentration of these two materials to maximize their ability to induce controlled polarity in EBs.

Gelatin and PEG are known to exhibit different bioactivities. The biodegradable gelatin is capable of mediating cell adhesion, proliferation and differentiation, while PEG hydrogels are nondegradable and chemically inert.[13] EBs were encapsulated in homogeneous PEG or GelMA hydrogels of various concentrations by UV photopolymerization.[14] As expected, EBs remained viable and proliferative after 6 days when encapsulated in GelMA with three different concentrations (5, 10, and 15 wt%). Interestingly, higher proliferation was observed for EBs encapsulated in lower concentrations of GelMA (**Figure 2A**). Our observation is in agreement with a number of previous studies in which encapsulation inside high concentrations of hydrogels reduced cell growth.[15] Interestingly, different degrees of EB sprouting were also observed when encapsulated in different concentrations of GelMA (Figure 2A). In low concentration GelMA (3 wt%), EBs exhibited distinct and robust sprouting that was reduced in GelMA with higher concentrations. The reduced proliferation and sprouting of EB in higher concentration of GelMA may be attributed to both the increased mechanical properties of the hydrogels and the enhanced spatial presence of the gelatin macromolecules required to be degraded for EB development.[15] Therefore both mechanical and biochemical properties of GelMA hydrogels may be contributing to EB sprouting.[16] EBs were able to maintain their viability upon encapsulation in the inert PEG hydrogels (Figure 2B), however much less cell proliferation was observed for EBs that were encapsulated in PEG than in GelMA hydrogels. Similarly, increased PEG concentration (15 wt%) reduced cell proliferation during 6 days of culture, while no EB sprouting was visible in PEG hydrogels which reaffirmed its biological inertness (Figure 2B). We did not test PEG hydrogels with concentrations lower than 10 wt%, since they were unstable in medium during long-term cell culture. We therefore chose 3 wt% GelMA and 10 wt% PEG to analyze the effect of hydrogels on EB differentiation.

Vasculogenic and cardiogenic differentiation in EB encapsulated in homogeneous GelMA (3 wt%) or PEG (10 wt%) hydrogels were investigated respectively after cultured in the same media used to form EBs (Figure 2C,D). Higher expression of vasculogenic cell genes, PECAM1 and Tie-2 was detected by RT-PCR in EBs encapsulated in GelMA than in PEG (Figure 2C). The elevated gene expression of PECAM1 and Tie-2 for EBs in GelMA and alpha-MHC for EBs in both PEG and GelMA is in agreement with previous studies which demonstrated that extracellular environment with high concentration of collagen promoted vasculogenic cell differentiation and cardiogenesis developed in early stage of embryo development.[5,17–19] We further characterized the protein expression of PECAM1 to confirm the pro-vasculogenic differentiation of EB in GelMA. As shown by immunostaining (Figure 2D), PECAM1 was highly expressed for the sprouting EBs encapsulated in GelMA, while weak expression of PECAM1 was detected only at the periphery of the EBs encapsulated in PEG. These results demonstrated the drastic difference between GelMA and PEG hydrogels in inducing EB development, which enabled us to explore their use for inducing EB polarity formation by patterning these two materials.

We induced polarization of individual EBs with spatially patterned vasculogenic differentiation by encapsulating individual

ADVANCED MATERIALS
www.advmat.de

www.MaterialsViews.com

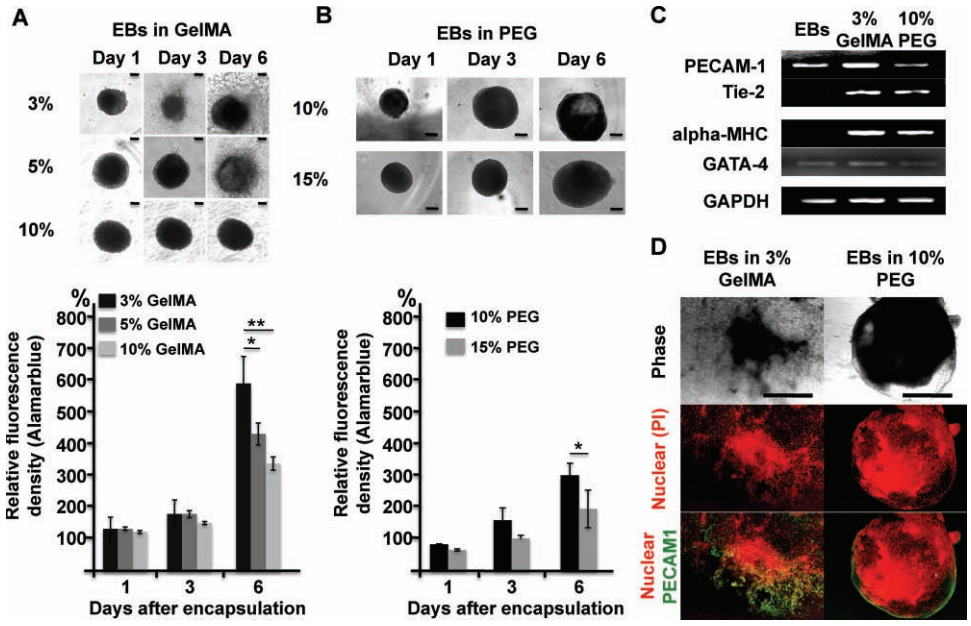

Figure 2. The effect of hydrogels properties on differentiation of EBs. (A,B) Phase contrast images of EBs at days 1, 3, 6. EBs were encapsulated in GelMA microgels with concentration of 3 wt%, 5 wt%, 10 wt% or PEG microgels with concentration of 10 wt%, 15 wt% respectively. Cell proliferation was measured by using Alamarblue assay at same time point and all data were normalized to day 0 values. ($n = 3$, * indicates $p < 0.05$, ** indicates $p < 0.01$). Scale bar: 300 µm. (C) Expression of vasculogenic (PECAM1, Tie2) and cardiogenic (alpha-MHC and Gata4) in EBs after 6 days in GelMA (middle lane), PEG (right lane) microgel, and in EBs before encapsulation (left line). (D) Immunostaining PECAM1 (green) (scanning confocal microscopy) in EBs encapsulated in 3 wt% GelMA (left lane) and 10 wt% PEG (right lane) after 7 days culture with nuclear co-staining (PI, red).

EBs inside microgels at an interface between 3 wt% GelMA and 10 wt% PEG. Using the above mentioned microengineering approach, arrays of EBs in GelMA/PEG hybrid microgels were generated with two halves of an individual EBs exposed to an asymmetrical matrix environment. The encapsulation of an individual EBs at the center of the 3D hybrid microgels (containing adjacent GelMA and PEG microgels) was illustrated by double staining of the two adjacent microgels (red for GelMA and green for PEG) and nuclear staining of EBs (**Figure 3A**). We cultured EBs encapsulated in the asymmetric microengineered matrices in the same media used for EBs forming. In these cultures sprouting was observed exclusively from the half of the EB that was encapsulated in the GelMA microgel. The degree of sprouts increased with culture time and became extensive by 7 days. In contrast, there was no visible morphological change in the other half of the EBs encapsulated in the PEG microgels, indicating that different cell-matrix interactions experienced by the two halves of the EB (Figure 3B left). The spatially patterned sprouting of individual EBs was verified by immunostaining of vasculogenic marker PECAM1, which marked the differentiated vasculogenic cells sprouting from EBs exclusively throughout the GelMA microgel (Figure 3B right). The patterned sprouting had extensive cell-matrix interactions between the EB and the GelMA microgel, which was illustrated by highly expression of vinculin, a protein in focal adhesion to mediate the cell-extracellular matrix interactions (Figure 3C left).[20] In agreement with PCR gene expression analysis no prominent vasculogenic differentiation was observed in the half EB encapsulated in the PEG microgel. To study the differentiation of EB exposed to GelMA/PEG hybrid microgels in real-time, we formed EBs from engineered ESCs carrying green fluorescent protein (GFP) at goosecoid (Gsc) gene locus. Gsc is an excellent marker for mesendoderm differentiation of ESCs, as it is expressed specifically in precursor cells from which definitive endoderm and mesodermal lineages arise.[21] After being cultured in the hybrid GelMA/PEG microgels for 7 days, EBs derived from the Gsc-GFP ESCs showed homogeneous GFP expression indicating mesendoderm differentiation of the entire EB (Figure 3C right) in comparison with EBs on day 1 after EB formation (data not shown). These results demonstrate that in GelMA/PEG hybrid microgels ESCs in EBs developed into vasculogenic cell lineages that sprouted into the GelMA microgels resulting in spatially asymmetrical patterns. Morphogen gradients have traditionally thought to be the major strategy for embryonic patterning. Here we showed that besides soluble factors, engineered asymmetrical matrices can also spatially pattern the differentiation of developing cells.

To further regulate the dynamics of vasculogenic patterning in individual EBs encapsulated in GelMA/PEG hybrid 3D microgels, we applied an extrinsic soluble factor. Marimastate, a broad-spectrum matrix metalloproteinase (MMP) inhibitor[22] was supplemented to culture medium to inhibit gelatin degradation. MMP is important for vascular cell invasion by degradation of surrounding extracellular matrix.[23] Therefore, we hypothesized that the addition of a MMP inhibitor should reduce vasculogenesis of EB encapsulated in the GelMA microgel. As expected, the sprouting of vascular network from EB in both the homogeneous GelMA microgel and in the GelMA/PEG hybrid microgel was significantly reduced in the presence of marimastate as illustrated by phase images and fluorescence

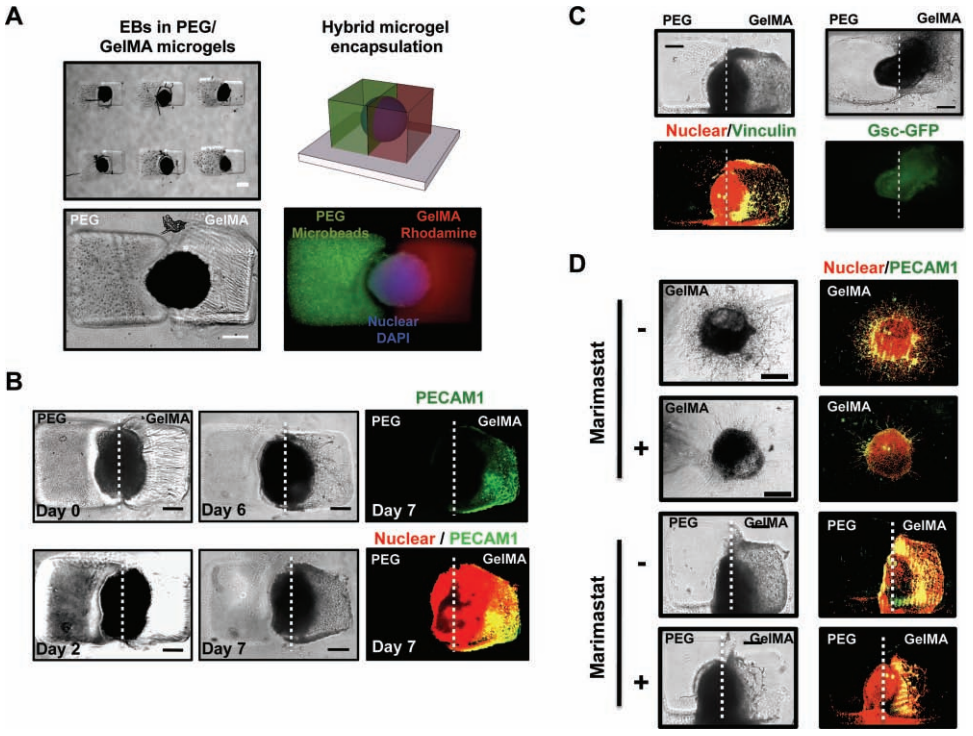

Figure 3. Polarity induction in individual EBs encapsulated in GelMA/PEG hybrid microgels with spatially-patterned vasculogenic differentiation. (A) Phase contrast images (left) of individual EBs in hybrid microgel. Microbead (green) laden PEG microgel and streptavidin conjugated Rhodamine (red) laden GelMA microgel in hybrid microgel structure and EB morphology stained by DAPI (right, blue). (B) Phase contrast image of EB during 7 days culture (left lanes), Immunostaining of PECAM1 (green) and PI (red) at day 7. (C) Immunostaining of vinculin (left); GFP labeled Gsc allele (right). (D) Regulating polarity formation of EB encapsulated in GelMA/PEG hybrid microgels by using soluble factor. Sprouting and PECAM1 expression (green) of EB encapsulated in homogeneous GelMA microgel (upper) and GelMA/PEG hybrid microgel (lower) were analyzed with and without supplement of MMP inhibitor marimastate. Nuclear was co-stained by PI (red). All scale bars: 300 μm.

immunostaining (Figure 3D). The ability to regulate the dynamics of polarity formation of EB enables the temporal control of the patterned differentiation, making our in vitro model more closely resembling the embryogenesis that is under well-orchestrated spatial and temporal regulation.

It is known that intercellular communication inside embryo is highly important in specifying patterning.[3,24] We therefore explored the possibility of similar intercellular communication within different portions of an individual EBs exposed to asymmetrical microenvironments. To do this, we quantified the area of the vasculogenic sprouting of EBs and correlated the area of EB sprouting with the spatial patterning of GelMA/PEG hybrid microgel with different ratios of the two materials. EB was virtually divided into 4 quarters as showed in schematics (**Figure 4K** upside). By adoption of the above mentioned patterning approach, each quarter of the EB was encapsulated in either GelMA or PEG microgel respectively resulting in GelMA/PEG hybrid microgels with ratios of 0:4, 1:3, 2:2, 3:1, and 4:0 (Figure 4A–E). After culturing cells for 7 days, vasculogenic sprouting of EB was imaged by immunostaining against PECAM1. As expected, vasculogenic cell in EB sprouted exclusively within GelMA microgels but not in PEG microgels. This behavior resulted in controlled sprouting patterns corresponding to GelMA/PEG ratios (Figure 4F–J). When we quantified the vasculogenic sprouting of EB represented by the PECAM1 immunostaining, significant differences in spatial patterns of vasculogenic sprouting were observed (Figure 4K). In particular we found that, quantitatively, the sprouting from each quarter of EB was determined not only by the hydrogels it directly interacted with, but also by the neighboring hydrogels environment. For example, in homogeneous GelMA microgel (with GelMA/PEG ratio of 4:0), the sprouting area from each quarter of EB was the largest (regarded as 100% sprouting); when one or more quarters of EB was encapsulated in PEG (with GelMA/PEG ratio of 3:1, 2:2, 1:3, or 0:4), not only the sprouting area from the regions encapsulated in PEG microgel was blocked (~20% for 3:1 and 2:2, below 5% for 1:3 and 0:4), but the sprouting area from the remaining quarters of EB encapsulated in GelMA was also reduced (~70% for 3:1 and 2:2 and ~25% for 1:3). These results showed that the presence of PEG played an inhibitory role to suppress the sprouting not only to the portion of the EB directly encapsulated within the PEG microgels, but also to EB regions encapsulated in adjacent GelMA microgels (Figure 4K). We observed that PEG inhibits sprouting of EBs in regions encapsulated in adjacent GelMA microgels. This effect may be due to intercellular cross-communication among different portions of individual EBs. It is known that diffusion of morphogens allow communication between different parts of the embryo and regulate differentiation event.[25] Here we hypothesize that secreted

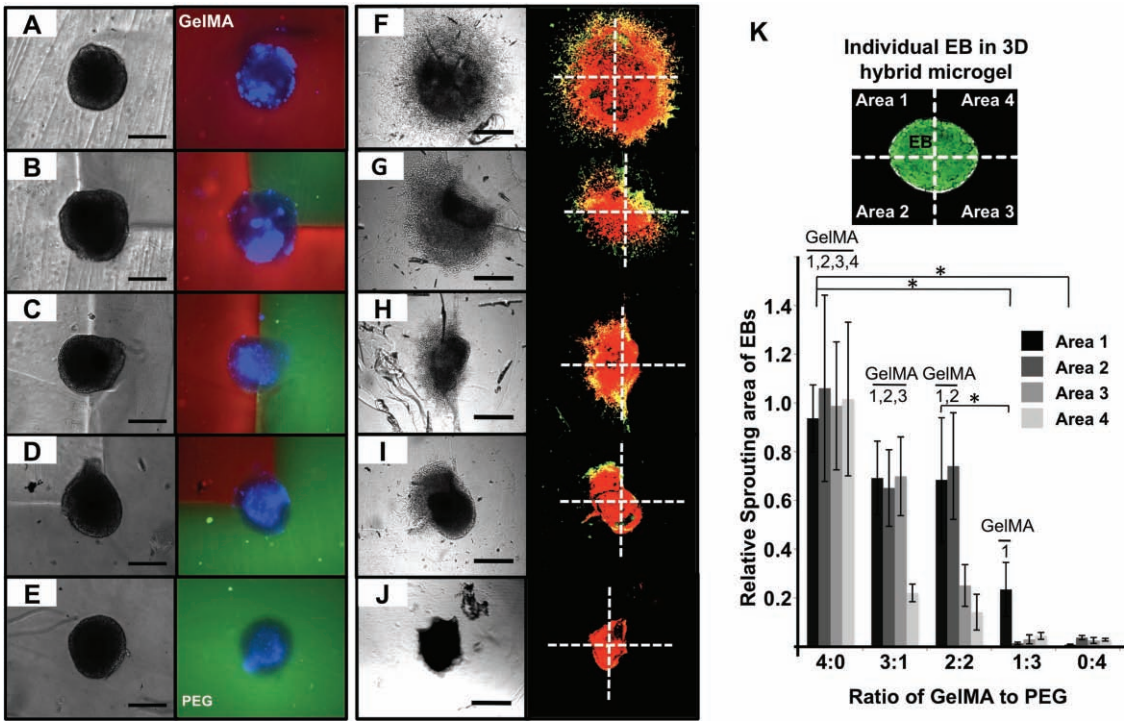

Figure 4. Spatial regulation of vasculogenic sprouting in GelMA/PEG hybrid microgels with various ratios of encapsulation materials. (A–E) Individual EBs were encapsulated in hybrid microgels with GelMA/PEG ratios of A = 4:0, B = 1:3, C = 2:2, D = 3:1, E = 0:4. GelMA or PEG microgel were precisely patterned with designated ratios and visualized in phase contrast images (left lane) and fluorescence images (right lane). For fluorescence imaging, PEG microgels were laden with fluorescent microbead (green) and GelMA microgel were laden with Rhodamine-labeled streptavidin (red) and EB was stained by DAPI (blue). (F–J) Phase contrast images of EBs after 7 days culture (left lane) and confocal fluorescent image of EBs stained with PECAM1 (green) and nucleus co-stained by PI (red, right lane). All scale bars: 500 μm. (K) Quantification of patterned vasculogenic sprouting area on each quarter of an individual EBs immunostained with PECAM1 and normalized to value of GelMA/PEG 4:0 sample as relative sprouting. Insert: Representation of four quarters of GelMA/PEG hybrid microgel where sprouting of EB was quantified within each individual quarter (* indicates $p < 0.05$).

factors diffuse through the EB, and that this secreted factors regulate the degree of endothelial cell development at an area being stimulated by GelMA. Moreover this inhibition of sprouting by PEG may be propagated and orchestrated within the entire EB. Thus, our results suggest that it may be possible to regulate cross-communication within an EB through precisely manipulating its microenvironment.

In summary, we developed a novel hybrid microgel platform containing asymmetrical extracellular matrices to mimic the anisotropic stem cell niche. The 3D hybrid microgels consist of two adjacent but independent parts made from two types of materials for inducing the patterned differentiation in individual EBs. As an example, spatially patterned vasculogenesis in individual EBs was achieved in GelMA/PEG hybrid microgels. Also the dynamics of vasculogenic patterns were shown to be controllable by the addition of soluble chemical factors. We further demonstrated that there may exist cross-communication within different portions of an individual EBs when encapsulated in different materials. The 3D spatial regulation on EB development by the asymmetrical microenvironments recapitulates some features of the polarized embryonic development. It is envisioned that this platform may be of benefit for mimicking asymmetrical environments to investigate spatially-regulated embryonic development. Furthermore, in tissue engineering studies, such approaches can be used to modulate the stem cell niche and provide powerful tools for generating patterned tissues to recreate complex organs.

Experimental Section

Encapsulation of individual EBs into GelMA/PEG hybrid microgels was performed within a microwell array by using the combination of micromolding and photolithography techniques. Wild type mouse ESC line R1 and engineered ESC line E14 encoding GFP at goosecoid (Gsc) gene locus were used for embryoid bodies formation. See main text and Supporting Information for details.

Acknowledgements

This research was funded by the US Army Engineer Research and Development Center, the Institute for Soldier Nanotechnology, the NSF CAREER Award, and NIH (EB008392, HL092836, DE019024). We would like to thank Drs. Ian Wheeldon, Jason Nichol and Jinhui Wu for scientific discussions.
H.Q. and Y.D. contributed equally to this work. H.Q., Y.D., and A.K. designed the research; H.Q. performed the experiments; L.W. and H.B. synthesized the materials; H.Q., Y.D., and H.K. analyzed the data; H.Q., Y.D., and A.K. wrote the paper.

Received: August 8, 2010
Published online: October 13, 2010

[1] A. Khademhosseini, R. Langer, J. Borenstein, J. P. Vacanti, *Proc. Natl. Acad. Sci. USA* **2006**, *103*, 2480.
[2] C. E. Murry, G. Keller, *Cell* **2008**, *132*, 661.
[3] D. ten Berge, W. Koole, C. Fuerer, M. Fish, E. Eroglu, R. Nusse, *Cell Stem Cell* **2008**, *3*, 508.
[4] I. S. Peter, E. H. Davidson, *Int. J. Dev. Biol.* **2009**, *53*, 707.
[5] R. S. Beddington, E. J. Robertson, *Trends Genet.* **1998**, *14*, 277.
[6] M. Zernicka-Goetz, *Development* **2002**, *129*, 815.
[7] G. Weitzer, *Handb. Exp. Pharmacol.* **2006**, 21.
[8] Y. S. Hwang, B. G. Chung, D. Ortmann, N. Hattori, H. C. Moeller, A. Khademhosseini, *Proc. Natl. Acad. Sci. USA* **2009**, *106*, 16978.
[9] S. Gerecht, J. A. Burdick, L. S. Ferreira, S. A. Townsend, R. Langer, G. Vunjak-Novakovic, *Proc. Natl. Acad. Sci. USA* **2007**, *104*, 11298.
[10] W. T. Fung, A. Beyzavi, P. Abgrall, N. T. Nguyen, H. Y. Li, *Lab Chip* **2009**, *9*, 2591.
[11] E. M. Lucchetta, J. H. Lee, L. A. Fu, N. H. Patel, R. F. Ismagilov, *Nature* **2005**, *434*, 1134.
[12] A. I. Van Den Bulcke, B. Bogdanov, N. De Rooze, E. H. Schacht, M. Cornelissen, H. Berghmans, *Biomacromolecules* **2000**, *1*, 31.
[13] A. S. Sawhney, C. P. Pathak, J. A. Hubbell, *Biomaterials* **1993**, *14*, 1008.
[14] N. E. Fedorovich, M. H. Oudshoorn, D. van Geemen, W. E. Hennink, J. Alblas, W. J. Dhert, *Biomaterials* **2009**, *30*, 344.
[15] J. W. Nichol, S. T. Koshy, H. Bae, C. M. Hwang, S. Yamanlar, A. Khademhosseini, *Biomaterials* **2010**, *31*, 5536.
[16] S. R. Peyton, C. B. Raub, V. P. Keschrumrus, A. J. Putnam, *Biomaterials* **2006**, *27*, 4881.
[17] H. Baharvand, A. Piryaei, R. Rohani, A. Taei, M. H. Heidari, A. Hosseini, *Cell Biol. Int.* **2006**, *30*, 800.
[18] J. M. Metzger, W. I. Lin, R. A. Johnston, M. V. Westfall, L. C. Samuelson, *Circ. Res.* **1995**, *76*, 710.
[19] S. J. Arnold, E. J. Robertson, *Nat. Rev. Mol. Cell Biol.* **2009**, *10*, 91.
[20] C. T. Mierke, P. Kollmannsberger, D. P. Zitterbart, G. Diez, T. M. Koch, S. Marg, W. H. Ziegler, W. H. Goldmann, B. Fabry, *J. Biol. Chem.* **2010**, *285*, 13121.
[21] S. Tada, T. Era, C. Furusawa, H. Sakurai, S. Nishikawa, M. Kinoshita, K. Nakao, T. Chiba, *Development* **2005**, *132*, 4363.
[22] F. Tsuji, K. Oki, A. Okahara, H. Suhara, T. Yamanouchi, M. Sasano, S. Mita, M. Horiuchi, *Cytokine* **2002**, *17*, 294.
[23] M. P. Lutolf, J. L. Lauer-Fields, H. G. Schmoekel, A. T. Metters, F. E. Weber, G. B. Fields, J. A. Hubbell, *Proc. Natl. Acad. Sci. USA* **2003**, *100*, 5413.
[24] C. Kiecker, C. Niehrs, *Development* **2001**, *128*, 4189.
[25] I. The, N. Perrimon, *Nat. Cell Biol.* **2000**, *2*, E79.